Sulfone Based-Electrolytes for Lithium-Ion Batteries: Cycling Performances and Passivation Layer Quality of Graphite and LiNi 1/3 Mn 1/3 Co 1/3 O 2 Electrodes

Benjamin Flamme, Jolanta Świątowska, Mansour Haddad, Phannarath Phansavath, Virginie Ratovelomanana-Vidal, Alexandre Chagnes

Journal of The Electrochemical Society

Sulfone Based-Electrolytes for Lithium-Ion Batteries: Cycling Performances and Passivation Layer Quality of Graphite and $LiNi_{1/3}Mn_{1/3}Co_{1/3}O_2$ Electrodes

Journal of The Electrochemical Society, 2020 **167** 070508

Sulfone Based-Electrolytes for Lithium-Ion Batteries: Cycling Performances and Passivation Layer Quality of Graphite and $LiNi_{1/3}Mn_{1/3}Co_{1/3}O_2$ Electrodes

Benjamin Flamme,[1] Jolanta Świątowska,[1,z] Mansour Haddad,[1] Phannarath Phansavath,[1] Virginie Ratovelomanana-Vidal,[1] and Alexandre Chagnes[2,z]

[1]*PSL Research University, CNRS-Chimie ParisTech, Institut de Recherche de Chimie Paris (IRCP), 75005 Paris, France*
[2]*Université de Lorraine, CNRS, GeoRessources, 54000 Nancy, France*

The solvent 3-methoxytetrahydrothiophene 1, 1-dioxide (MESL) was synthesized and its cycling performances of grapshite and $LiNi_{1/3}Mn_{1/3}Co_{1/3}O_2$ (NMC) electrodes were investigated in view of the high anodic stability of MESL in the presence of lithium bis-trifluoromethanesulfonimidate (LiTFSI). Galvanostatic charge-discharge of graphite electrode was possible in MESL + LiTFSI (1 M) only in the presence of 5% (vol.) fluoroethylene carbonate (FEC) at 40 °C. On the other hand, a good cycling ability of NMC electrode with this electrolyte was observed at room temperature even at a cut-off voltage of 4.5 V vs Li^+/Li. However, it was necessary to reduce the cut-off voltage from 4.5 V to 4.3 V vs Li^+/Li in order to keep a good cycling ability <<< when the temperature was increased from 25 °C to 40 °C due to an exaltation of oxidation reactions onto the cathode surface. X-Ray Photoelectron Spectroscopy (XPS) analyses were performed to investigate the electrode/electrolyte interphase and formation of passive layer on the electrode surfaces in order to explain the differences of cycling ability of NMC and graphite electrodes at room temperature and 40 °C.

 [DOI: 10.1149/1945-7111/ab63c3]

Manuscript submitted November 7, 2019; revised manuscript received December 9, 2019. Published January 10, 2020. *This paper is part of the JES Focus Issue on Challenges in Novel Electrolytes, Organic Materials, and Innovative Chemistries for Batteries in Honor of Michel Armand.*

For the last two decades, a large variety of batteries has been developed to respond to demand for various applications including cordless tools, data communication equipment, electric vehicles and renewable energy storage systems, etc.[1] The expected incssrease of electric vehicles production using LiBs technologyis is esstimated to be 7%–11% by 2025.[2] It will stimulate undoubtedly the research of new electrochemical storage technologies exhibiting high energy density. While many advances have been performed during the last decades on the development of new negative and positive electrodes in order to increase the charge-discharge capacity and the cycling ability of LiBs, less researches were devoted to the design of new liquid and solid electrolytes.[3–20]

Recently, our group published a review that gathers many data on the physicochemical and electrochemical properties of electrolytes for lithium-ion batteries.[4] This paper showed that seven families of dipolar aprotic organic solvent beside ionic liquids can be used in LiBs: carbonates, esters, ethers, acetals, sulfoxides, sulfites and sulfones. Each family presents advantages and disadvantages in terms of viscosity, ionic conductivity, thermal properties or anodic stability. Among these solvents, sulfones are an interesting in terms of thermal and oxidation stability except of viscosity, which remains too high and their ionic conductivities in the presence of lithium salt are usually very low. This review also showed that there is a great interest to extend the investigation of electrochemical and physicochemical properties to other sulfones in order to identify less viscous sulfones exhibiting higher ionic conductivities in the presence of lithium salts. Within this framework, a QSPR model was developed to find relationships between chemical structure and physicochemical properties of electrolytes.[21] For the first time, the physicochemical properties (dynamic viscosity, ionic conductivity, boiling and melting points) and the anodic stability of twenty-two new dipolar aprotic organic solvents bearing sulfone, ester and/or carbonate functions in the presence of lithium bis-trifluoromethanesulfonimidate (LiTFSI) were investigated by our group recently.[22] Among these molécules, the 3-methoxytetrahydrothiophene 1,1-dioxide (MESL) exhibited the most interesting anodic stability at a NMC electrode, i.e. 4.9 V vs Li^+/Li in the presence of 1 $mol \cdot l^{-1}$ LiTFSI.[22] Therefore, the present work deals with the investigation of the cycling ability of this new solvent in the presence of LiTFSI at graphite and NMC ($LiNi_{1/3}Mn_{1/3}Co_{1/3}O_2$) electrodes. The surface characterization was performed by X-ray Photoelectron Spectroscopy on the NMC and graphite electrodes as a function of cycling at different temperatures in order to understand the influence of passive layer and the influence of electrolyte decomposition on charge-discharge behavior.

[z]E-mail: jolanta.swiatowska@chimieparistech.psl.eu; alexandre.chagnes@univ-lorraine.fr

Material and Methods

Reagents.—Synthesis of MESL was performed according to the method reported in our previous work (Scheme 1).[21]

Fluoroethylene carbonate (Alfa Aesar, 99%) was used as received. An appropriate amount of lithium bis-trifluoromethanesulfonimidate (LiTFSI, Aldrich, Battery Grade) previously dried under vacuum at 120 °C overnight was dissolved in MESL to prepare the electrolyte at 1 $mol \cdot l^{-1}$. Water contents in electrolytes were measured by the coulometric Karl Fisher method by means of the Metrohm KF Titrando titrator. Water content was estimated at 20–30 ppm in the investigated sulfone-based electrolytes.

Galvanostatic charge-discharge tests.—The galvanostatic charge-discharge tests were carried out in Swagelok half-cells containing graphite electrode/Li (graphite was kindly provided by Saft) or NMC electrode/Li ($LiNi_{1/3}Mn_{1/3}Co_{1/3}O_2$, kindly provided by Pr. J.-M. Tarascon Lab at Collège de France) and two glass fiber separators (glass microfiber filter, 691, VWR, 11 mm diameter). The current collectors used during the tests were copper and aluminum discs for graphite and NMC electrodes, respectively. Swagelok assembly was carried out in an argon-filled glovebox containing less than 2 ppm H_2O and O_2.

During the galvanostatic charge-discharge tests, graphite electrodes were charged and discharged at a constant current to a cut-off voltage of 0.01 V and 2.5 V vs Li^+/Li, respectively. NMC electrodes were tested at constant currents up to discharge voltages of 4.5 V, 4.6 V or 4.7 V and charge voltage of 3 V vs Li^+/Li.

X-ray photoelectron spectroscopy.—X-ray photoelectron spectroscopy was used to analyze the surface composition of graphite and NMC electrodes after cycling in MESL-based electrolytes. VG

Scheme 1. Synthetic pathway used for MESL.

ESCALAB 250 spectrometer was employed for X-Ray Photoelectron Spectroscopy (XPS) surface chemical characterization of electrode materials (NMC and graphite) before and after cycling. The graphite and NMC electrodes underwent five charge-discharge cycles at room temperature and 40 °C between 2.5 V and 0.01 V vs Li^+/Li (C/20) and between 4.5 V and 3 V vs Li^+/Li (C/20), respectively. After galvanostatic cycling, the electrodes were removed from the Swagelok cell, rinsed with DMC and dried in the glove box before being introduced into the XPS analysis chamber using an anhydrous and anaerobic transfer system as previously reported.[23]

Al Kα monochromatized radiation ($h\upsilon = 1486.6$ eV) was used as the X-ray source. The spectrometer was calibrated against the reference binding energies (BE) of Cu (932.6 eV), Ag (368.2 eV) and Au (84 eV) samples. All analyses were performed in the analysis chamber (pressure $\sim 10^{-9}$ mbar) at a take-off angle of 90°. High resolution spectra (C 1s, F1s, S 2p) were collected with a pass energy of 20 eV. Binding energies of the component peaks were corrected with reference to the –CH–CH– set at 285.0 eV. Peak fitting and decomposition were performed with the Advantage software version 5.966 provided by Thermo Electron, using a Shirley-type background and Gaussian/Lorentzian peak shapes at a fixed ratio of 70/30. The experimental and fitted curves are included in the figures presenting the XPS results.

Results and Discussion

Charge-discharge tests of graphite electrode.—Preliminary tests showed an important fading at the graphite electrode throughout the charge-discharge cycles when MESL + 1 mol l^{-1} LiTFSI was used as electrolyte (fading of 90% after 50 cycles between 2.5 and 0.01 V vs Li^+/Li at room temperature).

Fluoroethylene carbonate (FEC) was added into the electrolyte as this additive usually improves the coulombic efficiency and capacity retention of negative electrodes including graphite and Si-based electrodes by forming an efficient solid electrolyte interphase layer (SEI) onto the electrode surface.[24–26] Figure 1 shows that the addition of 1% (vol.) FEC in MESL + 1 mol l^{-1} LiTFSI improved cycling ability of the graphite electrode. The low coulombic efficiency observed at the first cycle results from electrolyte reduction onto the graphite surface as very often observed for negative electrodes.[27–31] However, after the first cycle, the coulombic efficiency is close to 100% due to the passive film already formed, which avoids further electrolyte reduction.

A small increase of the charge-discharge capacity was obtained by increasing FEC concentration from 1% (vol.) to 5% (vol.) as illustrated in Fig. 2. The low coulombic efficiency during the first cycle is related to the important electrolyte decomposition and formation of SEI layer as in the case discussed above (Fig. 1). However, during the following cycles, the high values of coulombic efficiency after the first cycle (≈100%) shows that SEI layer formed onto the electrode surface was stable and was not re-dissolved during lithium deinsertion.

The low value of the charge-discharge capacity (160 mAh g^{-1} instead of 330 mAh g^{-1} as theoretically expected) may be explained by:

- the formation of the bad quality SEI layer (composition and/or thickness) exhibiting high impedance,
- the difficulties of electrolyte penetration into the graphite pores because of the high viscosity of sulfone-based electrolytes (a recent study showed that the dynamic viscosity of 3-ethoxytetrahydrothiophene 1,1-dioxide, which the chemical structure is very close to MESL, is equal to 19.1 cP at 25 °C).[22]

Figure 3 shows the influence of charge-discharge rates on capacity and coulombic efficiency of graphite electrode cycled in 1 mol l^{-1} LiTFSI in MESL in the presence of 5% (vol.) FEC at 40 °C.

Comparison of charge and discharge capacities at room temperature (Fig. 2) and 40 °C (Fig. 3) for a charge-discharge rate of C/20 shows that an increase of the temperature was responsible for an increase of the charge-discharge capacities without affecting the coulombic efficiency or the irreversibility. Therefore, the low capacity observed in Figs. 1–2 may result from the high viscosity of the electrolyte at low temperatures. The higher the temperature, the lower the viscosity is, and the better the electrolyte penetration into the electrode porosity.[19]

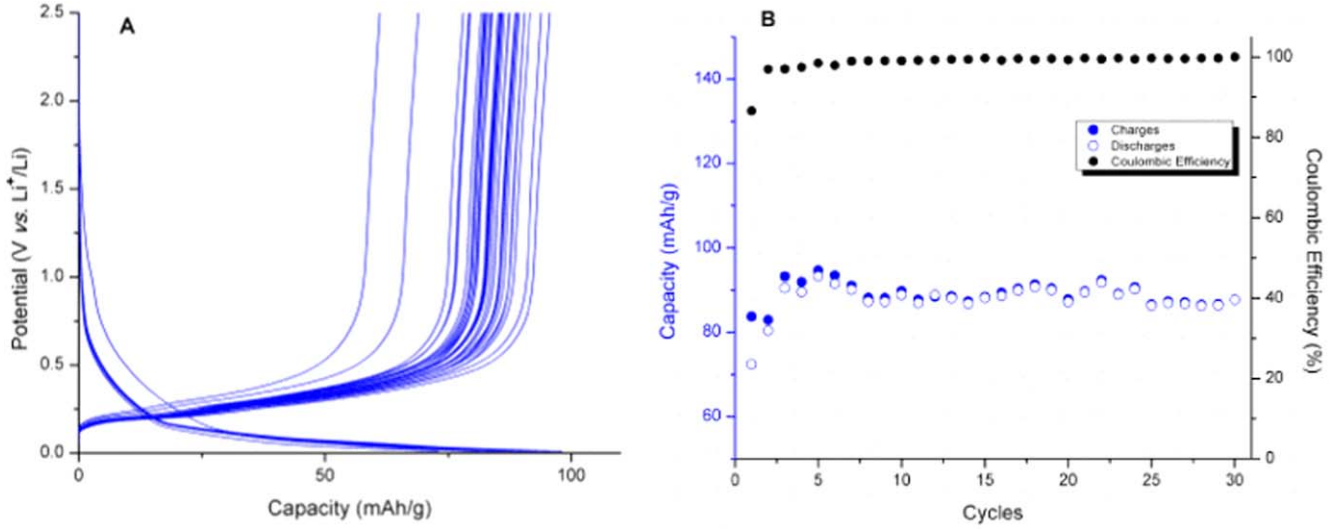

Figure 1. (a) Galvanostatic charge-discharge tests for a graphite electrode cycled at C/20 at room temperature in 1 mol l^{-1} LiTFSI in MESL in the presence of 1% (vol.) FEC and (b) corresponding variations of specific capacities and coulombic efficiency.

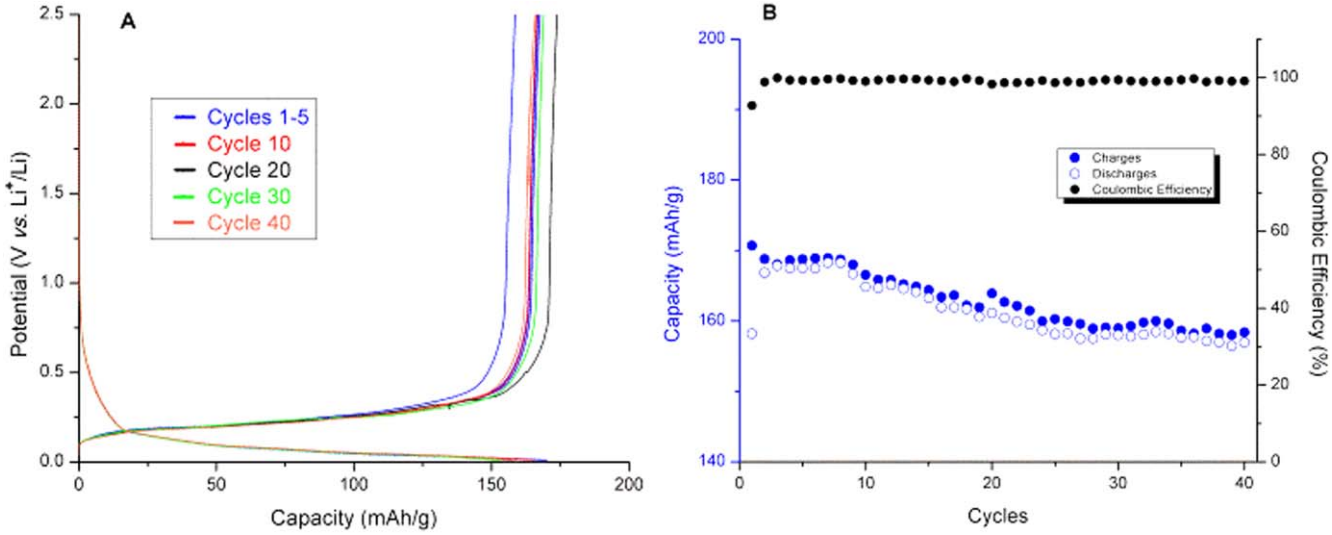

Figure 2. (a) Galvanostatic charge-discharge tests for a graphite electrode cycled at C/20 at room temperature in 1 mol l^{-1} LiTFSI in MESL in the presence of 5% (vol.) FEC and (b) corresponding variations of specific capacities and coulombic efficiency.

Charge-discharge tests of NMC electrode.—Preliminary tests showed an important capacity loss of NMC electrode in MESL + 1 mol l^{-1} LiTFSI at room temperature between 3 and 4.5 V vs Li^+/Li. The addition of 1% (vol.) FEC enhanced slightly the cycling ability of NMC. A significant improvement of the cycling ability of NMC electrode in MESL-based electrolyte was obtained in the presence of 5% (vol.) FEC in comparison to 1% (vol.) FEC (Fig. 4).

In the presence of 1% (vol.) FEC, the initial charge-discharge capacities were around 80 mAh g^{-1} and the fading was of 3% per cycle while coulombic efficiencies were comprised between 85% and 90% during the first five cycles and remained constant around 95% during the next 25 cycles. In the presence of 5% (vol.) FEC, the coulombic efficiencies were close to 100% after 30 cycles and the fading was only equal to 0.7% per cycle.

Figure 5 shows floating tests for NMC electrode performed at room temperature and 40 °C in MESL + 1 mol l^{-1} LiTFSI with 0% and 5% (vol.) FEC.

It can be observed that FEC decreases the electrolyte oxidation since current was drastically reduced in the presence of FEC (Fig. 5a). FEC does not prevent the electrolyte oxidation but it leads to its significant decrease. However, a temperature increase to 40 °C (Fig. 5b) shows a significant current increase, which can be attributed to a strong decrease of the anodic stability of the electrolyte.

Figure 6 shows the variations of NMC capacity@ and coulombic efficiency as a function of charge-discharge cycles in MESL + 5% (vol.) FEC + 1 mol l^{-1} LiTFSI at 40 °C and room temperature.

Side reactions occur due to the low anodic stability of the electrolyte at 40 °C. The dramatic decrease of coulombic efficiency and charge-discharge capacity are due to exaltation of electrolyte reduction at 40 °C. A decrease of the temperature improves markedly the coulombic efficiency and cycling ability of the electrode. At room temperature, there is no significant electrolyte oxidation and NMC can be cycled. However, fading was still too high, and the charge-discharge capacity was still lower than the theoretical value to envisage any applications of NMC and MESL-FEC-LiTFSI electrolyte in high-voltage LiBs. Cycling ability behavior may be enhanced by adding a co-solvent exhibiting low viscosity and increasing the anodic stability. Esters could be one of such candidates given that their viscosities are significantly lower than those obtained in electrolytes containing sulfone.[4]

Surface characterization.— *NMC electrode cycled in MESL based electrolyte.*—XPS analyses were performed on the pristine

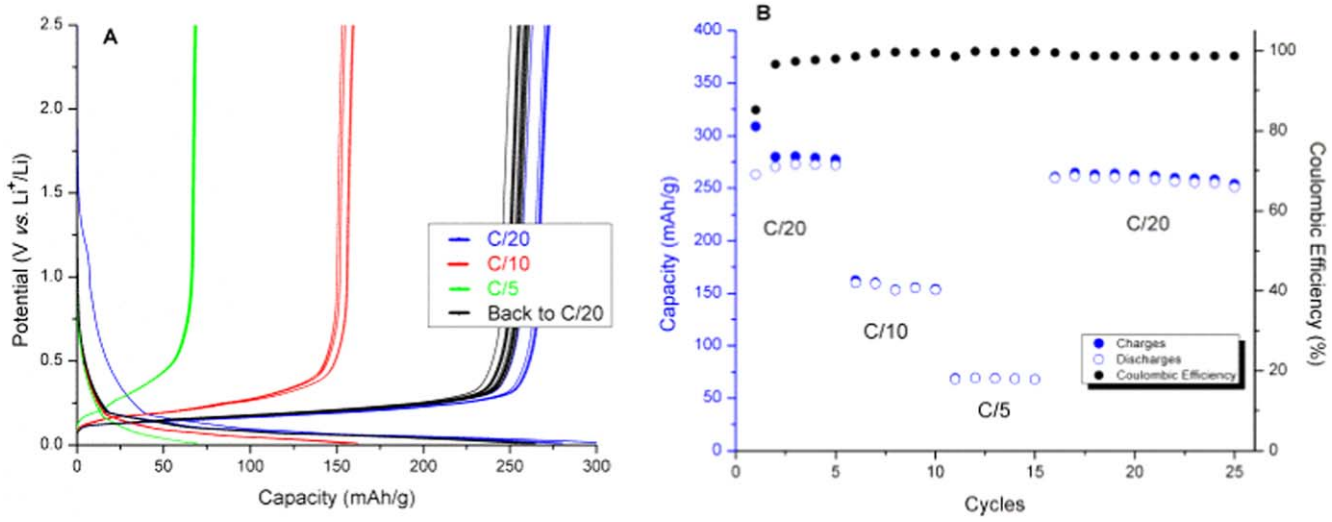

Figure 3. (a) Galvanostatic charge-discharge tests for a graphite electrode performed at 40 °C in 1 mol l^{-1} LiTFSI in MESL in the presence of 5% (vol.) FEC performed at different rates: C/20, C/10, C/5 and C/20 and (b) corresponding variations of specific capacities and coulombic efficiency.

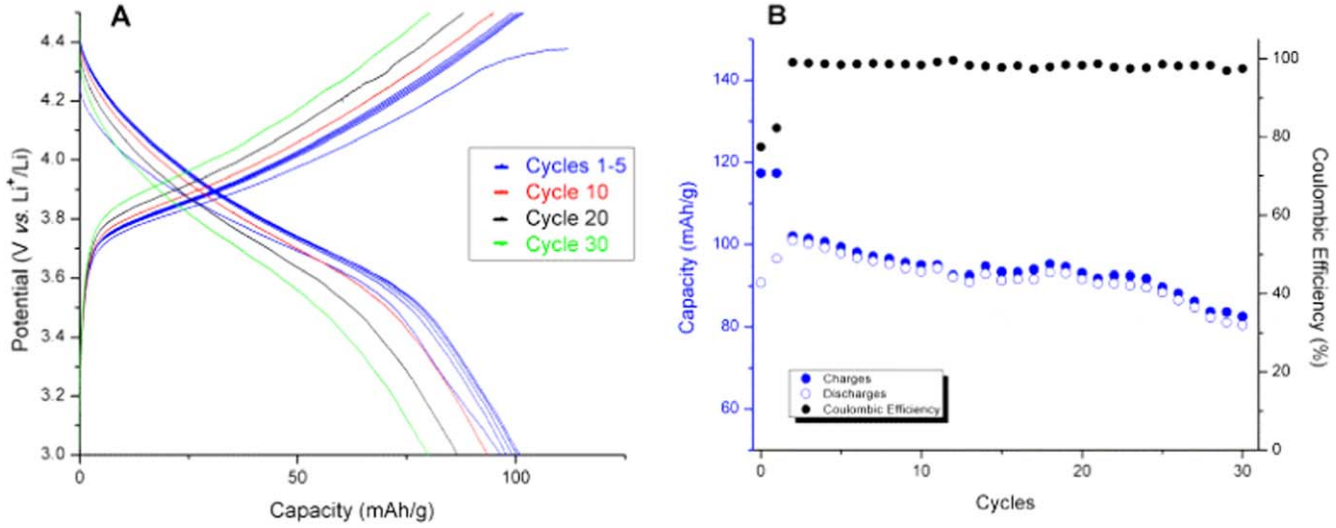

Figure 4. (a) Galvanostatic charge-discharge tests for NMC electrode performed at C/20 at room temperature in 1 mol l^{-1} LiTFSI in MESL in the presence of 5% (vol.) FEC and (b) corresponding variation of specific capacities and coulombic efficiency. Discharge performed down to a cut-off voltage of 4.5 V and charge to a cut-off voltage of 3 V vs Li^+/Li.

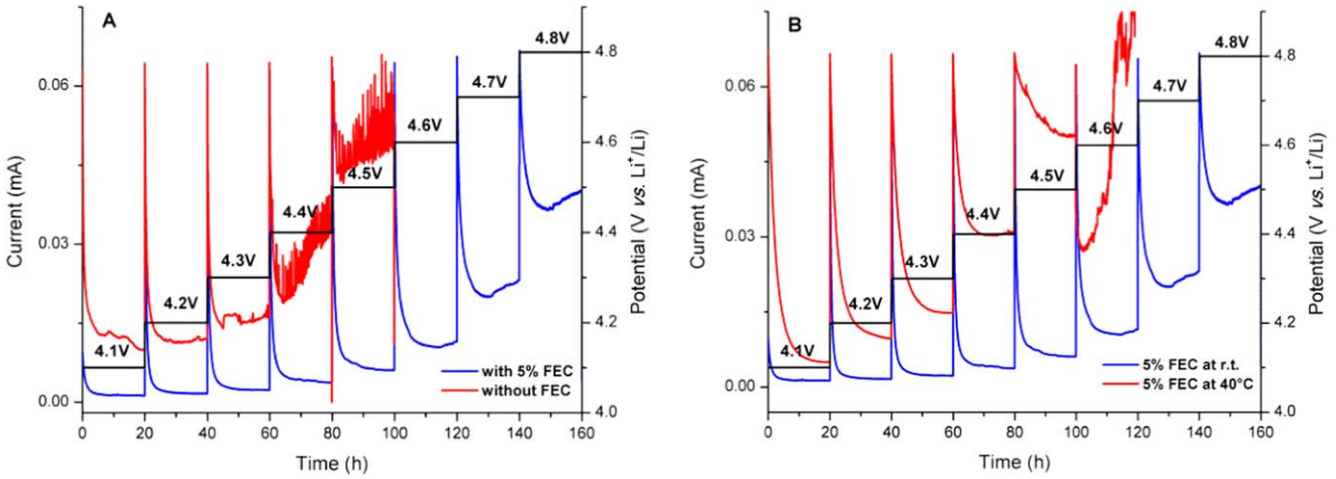

Figure 5. Floating tests performed for NMC electrode in MESL + 1 mol l^{-1} LiTFSI without and with 5% (vol.) FEC at room temperature (a) and in the presence of 5% (vol.) FEC at room temperature and at 40 °C (b). The floating tests were performed during 20 h at constant voltage comprised between 4.1 V and 4.8 V vs Li^+/Li.

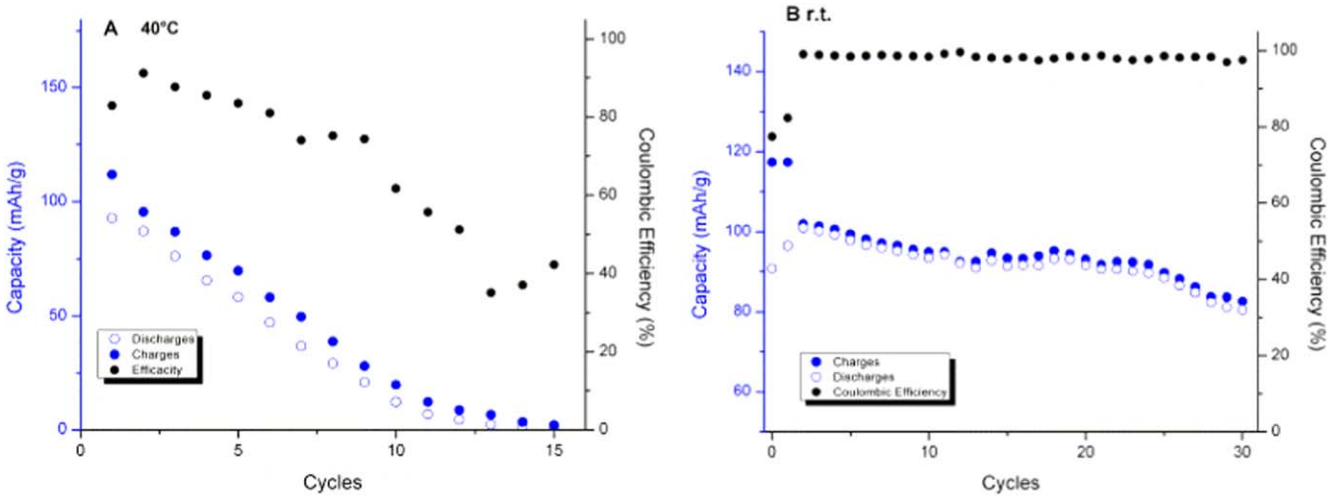

Figure 6. Specific charge-discharge capacities and coulombic efficiencies of NMC electrode cycled in MESL + 1 mol l^{-1} LiTFSI in the presence of 5% (vol.) FEC: (a) at 40 °C and (b) at room temperature. Charge-discharge rate = C/20 and D/20 performed at constant current; discharge performed down to a cut-off voltage of 4.5 V and charge up to a cut-off voltage of 3 V vs Li^+/Li.

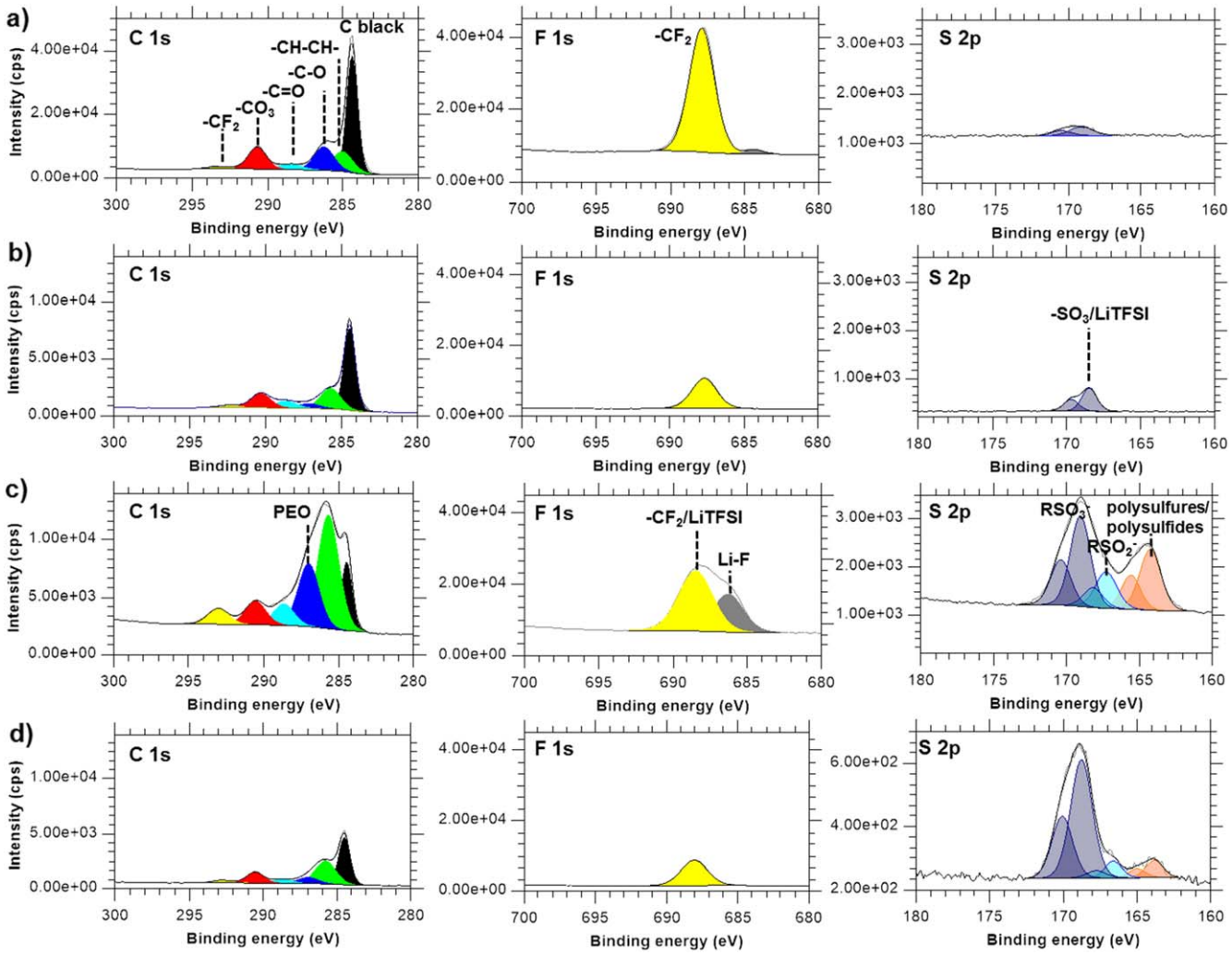

Figure 7. C 1s, F 1s and S 2p core level peaks obtained on the pristine NMC electrode (a) and after 5 cycles of charge-discharge at C/20 in MESL + LiTFSI electrolyte without (b) and with FEC (5%) additive at room temperature (c) and 40 °C (d).

NMC electrode and after 5 cycles of charge-discharge performed in MESL + LiTFSI with or without FEC (5%) at room temperature and 40 °C (Fig. 7). Only the principal peaks (C 1s, F 1s, S 2p) corresponding to the electrolyte decomposition and formation of the passive layer are presented here. The Ni 2p, Mn 2p and Co 2p core level signals (not presented here) corresponding to the NMC electrode material show a small intensity decrease after cycling in MESL + LiTFSI without FEC and a significant intensity decrease after cycling in MESL + LiTFSI + FEC. This signal attenuation of the Ni 2p, Mn 2p and Co 2p peaks can be attributed to SEI formation on the NMC electrode. XPS analyses show that there was no change in the oxidation state of nickel, manganese or cobalt. The small signal attenuation of Ni 2p, Mn 2p and Co 2p peaks observed after cycling NMC in MESL + LiTFSI without FEC is attributed to non-significant surface modifications, which can be confirmed by some negligible changes in the C 1s, F 1s and S 2p signals towards the non-cycled pristine NMC electrode (Fig. 7). The C 1s core level signal for the pristine NMC electrode (Fig. 7a) presents six peaks, which can be attributed to: carbon black at 284.4 eV, –CH–CH– at 285.0 eV (PVDF), –C–O at 286.3 eV, –C=O at 288.5 eV, $–CO_3$, at 290.7 eV and $–CF_2$ (PVDF) at 293.2 eV. The F 1s peak at 688.0 eV corresponding to the $–CF_2$ bonding can be attributed to the PVDF binder present in the NMC composite electrode material as already observed in the C 1s peak.[17,32,33] Only small intensity S 2p peak at 169.1 eV can be observed on the pristine NMC electrode showing a negligible surface contamination by sulfur species originating from handling of the electrode.

After NMC cycling in MESL + LiTFSI without FEC, the C 1s and F 1s peaks do not show considerable changes (Fig. 7b). Peaks attributed to carbon black and PVDF binder can be clearly observed, which indicates a formation of thin passive layer not leading to attenuation of peaks identified in the bulk composite electrode material. More significant changes can be observed in the case of S 2p signal showing significantly higher intensity than on the pristine electrode. The S 2p peak is composed of closely spaced spin-orbit components S $2p_{3/2}$ and S $2p_{1/2}$ (with $\Delta = 1.16$ eV) (Fig. 7b). The principal S $2p_{3/2}$ peak observed at 168.4 eV attributed to $–SO_3$ can originate from the presence of MESL decomposition products or the presence of Li-imide salt (LiTFSI) or its decomposition products.[34]

The cycling of NMC electrode at room temperature in MESL + LiTFSI + FEC has an important influence on the surface modifications (Fig. 7c). The peaks corresponding to NMC electrode as well as carbon black and PVDF binder are significantly attenuated indicating the formation of thicker and/or more homogenous surface layer than on the electrode cycled without FEC. The results of electrolyte decomposition can be evidenced by a strong intensity increase of the peak located at 285.6 eV corresponding to C–C/C–H bonding, and the second one at 287.0 eV corresponding to –C–O–C– bonding, i.e. polymeric compound such as poly(ethylene oxide) PEO

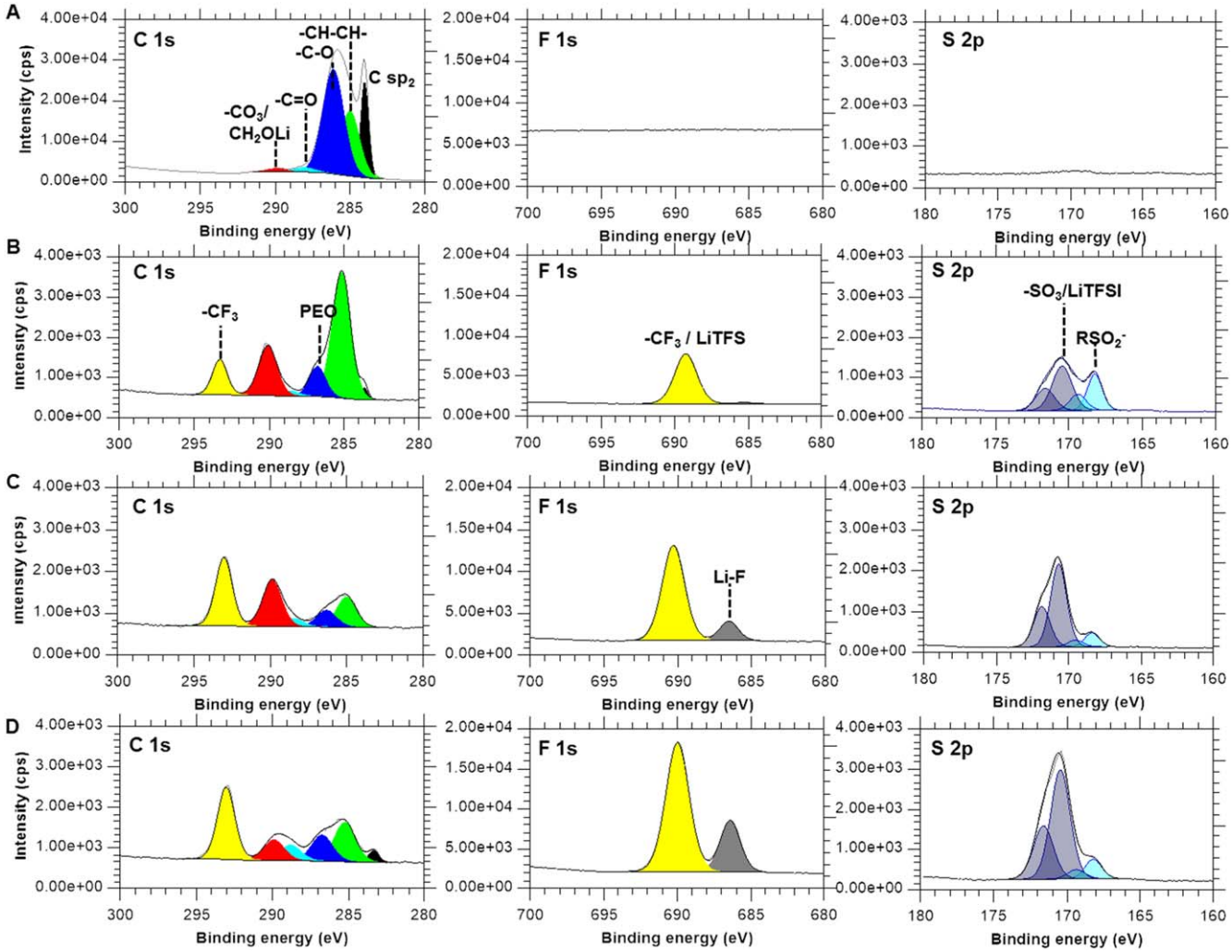

Figure 8. C 1s, F 1s and S 2p core level peaks obtained on the pristine graphite electrode (a) and after 5 cycles of charge-discharge at C/20 in MESL + LiTFSI electrolyte without (b) and with FEC (5%) additive at room temperature (c) and 40 °C (d).

((–CH_2–CH_2–O–)n).[28] The other components comprised in C 1s region are not significantly modified with reference to the C 1s peaks obtained on the pristine NMC surface or on the NMC surface after cycling in MESL + LiTFSI without FEC. Significant modifications of F 1s core level peak are observed since two well distinguished peaks appear at 686.3 eV and 688.5 eV attributed to Li-F and to –CF_2 or to Li-imide salts (LiTFSI) or their decomposition products, respectively.[17,28,35] The high intensity peak at 688.5 eV cannot justify only the presence of –CF_2 bonds since the C:F ratio of C and F peaks is not exactly equal to 2 (stoichiometry of –CF_2). Thus, it can be concluded that other species such as LiTFSI or their products of decomposition were present on the NMC surface. Much more important modifications can be observed in the case of S 2p core level peak where three contributions can be identified at 164.2, 167.3 and 169.0 eV, which may correspond to polysulfures/polysulfides, –SO_2 (RSO_2–) and –SO_3/–SO_4 (RSO_3–), respectively. These results are coherent with the detection of similar compounds on the surface of $Li_7Ti_5O_{12}$ electrode cycled in electrolytes containing sulfones such as EMS and TMS.[36] The presence of sulfur-containing species was also observed in the surface layer formed on other active electrode materials.[37] Cycling in sulfone-based electrolytes can lead to Li_2SO_3 and RSO_3Li formation as evidenced previously on graphite and NMC surface.[38,39] However, it should be also noted that the presence of sulfur-containing species can be also related to LiTFSI decomposition leading to Li_2SO_3 and polysulfures/polysulfides formation.[40–42] Nonetheless, the three S $2p_{3/2}$ peaks may result from the presence of MESL solvent and LiTFSI salt, and their products of decomposition since cycling in EMS-based electrolytes showed principally the formation of (RSO_2–) and (RSO_3–) and not the presence of polysulfures/polysulfides.[34]

After NMC cycling at 40 °C in MESL + LiTFSI + FEC (Fig. 7d), the thickness or the homogeneity of the passive layer onto the electrode surface was significantly decreased towards the SEI layer formed on the electrode cycled at room temperature. This can be concluded from the high intensity of the C 1s peak corresponding to the black carbon at 284.6 eV and lower intensity peaks located at higher binding energies corresponding to electrolyte decomposition. The formation of thinner or non-homogeneous passive layer is also confirmed by the presence of higher intensity Ni 2p, Mn 2p and Co 2p peaks (not shown here) when the electrode was cycled at 40 °C in comparison the the NMC electrode cycled at room temperature. It should be emphasized that little attention has been paid to investigate the influence of additive on the formation of the SEI layer on positive electrode materials. According to our knowledge there is no study regarding the influence of additives in sulfone-based electrolytes.

The presence of a unique F 1s peak at 688.1 eV attributed to PVDF after cycling the NMC electrode at room temperature or 40 °C in MESL-LiTFSI indicates the absence of inorganic products of salt decomposition. However, it should be noticed that the lower intensities of sulfur peaks can indicate the impoverishment of the surface layer in sulfur species. Furthermore, high temperature leads

to partial dissolution and formation of more heterogeneous surface layer, which leads to fast capacity decrease and low columbic efficiency. Less stable and less homogenous layer can be also a reason of slight dissolution and cleavage of NMC compounds of electrode materials. The addition of FEC may also inhibit electrode degradation.[43]

Graphite electrode cycled in MESL based electrolyte.—Slightly different surface layer was formed on the graphite electrode. Figure 8 presents the C 1s, F 1s and S 2 p core level peaks obtained by XPS analysis of a graphite electrode after 5 charge-discharge cycles at C/20 between 2.5 V and 0.01 V in MESL + LiTFSI without and with FEC (5% vol.) at room temperature and 40 °C.

The SEI layer formed on the graphite electrode is thicker and/or more homogenous than the passive layer formed on the NMC surface since the peak intensity at 284.6 eV corresponding to carbon sp2 bonding is lower on the graphite electrode than on the NMC electrode after cycling in MESL + LiTFSI electrolyte without FEC additive (Fig. 8b). The passivation of the positive electrode is usually less significant because electrolyte stability at high potential is theoretically greater than at low potential.[44–48] The attenuation of the peak corresponding to graphite (at 284.6 eV) is accompanied by a significant increase of the highest binding energy peaks at 290.4 and 293.9 eV corresponding to $–CO_3$/$–CH_2OLi$ and $–CF_3$, respectively. More important intensity increase of these two peaks can be observed for the graphite cycled in MESL-LiTFSI-FEC at room temperature and 40 °C (Figs 8c and 8d, respectively). Moreover, the addition of FEC in MESL-LiTFSI was responsible for an increase of –C–O–C– peak at 286.6 eV attributed to the presence of polymeric compounds such as poly(ethylene oxide) PEO ((–CH_2–CH_2–O–)n).[28]

The presence of $–CF_3$ clearly evidenced by the C 1s and F 1s regions (peaks at 293.7 ± 0.2 eV and 689.5 ± 0.2 eV, respectively) can be explained by decomposition of LiTFSI salt, which was addressed in previous studies.[49,50] The salt degradation can be also confirmed by the presence of N 1s (not shown here) and S $2p_{3/2}$ at around 168.3 (±0.2) eV. As demonstrated by the significant intensity of the F 1s peak located at 168.3 (±0.2) eV and the C1s peaks located at 293.7 ± 0.2 eV (Fig. 8), the decomposition of LiTFSI was much more important on the graphite surface than on the NMC surface (Fig. 7).

Concerning the S $2p_{3/2}$ peak observed after cycling the graphite electrode in MESL + LiTFSI without or with FEC at room temperature and 40 °C (Figs 8c and 8d, respectively), only two peaks can be observed at 168.4 (±0.2) eV and 170.4 (±0.2) eV, which correspond to $–SO_2$ (RSO_2–) and $–SO_3$/$–SO_4$ (RSO_3–), respectively. The lower binding energy peak observed for NMC electrode at around 164.2 eV corresponding to polysulfures/polysulfides was not observed. As mentioned above, the presence of polysulfures/polysulfides can result from LiTFSI decomposition. It can be then concluded that RSO_2– and RSO_3– arising from MESL decomposition onto the graphite surface may contribute to the formation of a relatively stable SEI layer. Therefore, the increase of the temperature (i) improved the cycling ability because of easier electrolyte diffusion into the electrode pores, and (ii) enhanced the formation of a good quality solid electrolyte interface layer with slightly lower thickness and lower enrichment in $–CO_3$/$–CH_2OLi$ species. Such a SEI layer seems to have the optimal properties in order to protect the graphite electrode against exfoliation and to allow the reversible lithium insertion into the graphene layers.

Conclusions

MESL exhibits high anodic stability but it cannot be utilized as a pure solvent due to its low ability to form a good quality SEI layer onto graphite and NMC electrodes.

The low cycling performances of NMC electrode between 2.5 V and 4.5 V vs Li^+/Li at 40 °C was observed due to exaltation of electrolyte oxidation at NMC electrode at 40 °C while good performances were observed at room temperature. Thin SEI layer on NMC enriched in S species originating from MESL decomposition products or Li-imide salt (LiTFSI) was observed by XPS. However, it seems that in the absence of FEC the contribution of LiTFSI in SEI composition is less significant than MESL contribution, which tends to oxidize onto the NMC surface, especially at high potentials. The addition of FEC led to a significant increase of the SEI thickness, with formation of new C and F-like species on the electrode surface (as shown by XPS) likely improving the SEI homogeneity. However, at higher temperature (40 °C) the SEI thickness was reduced on NMC electrode, leading to lower cycling performances, even with the addition of FEC, which may inhibit electrode degradation.

Nonetheless, good cycling ability of graphite electrode cannot be achieved at room temperature due to sluggish electrolyte diffusion into the pores of graphite since MESL is highly viscous. An increase of the temperature to 40 °C resulted in reducing electrolyte viscosity and, therefore, enhanced electrolyte diffusion. Besides of increased electrolyte diffusion into the graphite, XPS characterization performed on the graphite electrode showed that at higher temperatures the formation of good quality SEI layer is possible with a lower thickness and slightly different composition (lower quantity of $–CO_3$/$–CH_2OLi$ species).

As a conclusion, these results show that MESL/FEC + LiTFSI electrolyte can be viewed as a relevant electrolyte providing that the formulation would be improved by adding a low viscous solvent exhibiting high anodic stability in order to obtain good cycling performances at room temperature without any issues. Preliminary experiments led to the conclusion that ether could be a relevant co-solvant.

Acknowledgments

The authors thank the Agence Nationale de la Recherche for financial support (ANR DEVEGA, N°ANR-14-CE05-0001-01).

References

1. A. Chagnes, in *Lithium Process Chemistry: Resources, Extractions, Batteries and Recycling*, ed. A. Chagnes and J. Swiatowska (Elsevier, Amsterdam) pp 41–80 (2015).
2. Nickel la revue spécialisée et ses applications, Vol. 32, Iss. 1 (2017), https://www.nickelinstitute.org/nickel-magazine/nickel-magazine-vol-32-no-1-2017/.
3. A. Varzi, R. Raccichini, S. Passerini, and B. Scrosati, "Challenges and prospects of the role of solid electrolytes in the revitalization of lithium metal batteries." *J. Mater. Chem. A*, **4**, 17251 (2016).
4. B. Flamme, G. Rodriguez Garcia, P. Phansavath, V. Ratovelomanana-Vidal, and A. Chagnes, "Guidelines to design organic electrolytes for lithium-ion batteries: environmental impact, physicochemical and electrochemical properties." *Green Chem.*, **19**, 1828 (2017).
5. J. Ming et al., "New insight on the role of electrolyte additives in rechargeable lithium ion batteries." *ACS Energy Lett.*, **4**, 2613 (2019).
6. X. B. Kong, R. Zhou, J. Wang, and J. B. Zhao, "An effective electrolyte strategy to improve the high-voltage performance of $LiCoO_2$ cathode materials" *ACS Appl. Energy Mater.*, **2**, 4683 (2019).
7. C. C. Su, M. N. He, R. Amine, Z. H. Chen, R. Sahore, N. D. Rago, and K. Amine, "Cyclic carbonate for highly stable cycling of high voltage lithium metal batteries." *Energy Storage Mater.*, **17**, 284 (2019).
8. I. Geoffroy, A. Chagnes, B. Carré, D. Lemordant, P. Biensan, and S. Herreyre, "Electrolytic characteristics of asymmetric alkyl carbonates solvents for lithium batteries." *J. Power Sources*, **112**, 191 (2002).
9. H. Lyu, Y. C. Li, C. J. Jafta, C. A. Bridges, H. M. Meyer, H. M. A. Borisevich, M. P. Paranthaman, S. Dai, and X. G. Sun, "Bis(trimethylsilyl) 2-fluoromalonate derivatives as electrolyte additives for high voltage lithium ion batteries." *J. Power Sources*, **412**, 527 (2019).
10. J. E. Morales-Ugarte, E. Bolimowska, H. Rouault, J. Santos-Pena, C. C. Santini, and A. Benayad, "EIS and XPS Investigation on sei layer formation during first discharge on graphite electrode with a vinylene carbonate doped imidazolium based ionic liquid electrolyte." *J. Phys. Chem. C*, **32**, 18223 (2018).
11. A. Chagnes, H. Allouchi, B. Carré, G. Oudou, P. Willmann, and D. Lemordant, "γ-Butyrolactone-ethylene carbonate-based electrolytes for lithium-ion batteries." *J. Appl. Electrochem.*, **33**, 589 (2003).
12. A. Chagnes, B. Carré, P. Willmann, R. Dedryvère, D. Gonbeau, and D. Lemordant, "Cycling ability of γ-butyrolactone-ethylene carbonate based electrolytes." *J. Electrochem. Soc.*, **159**, A1255 (2003).
13. C. Y. Wang, L. Yu, W. Z. Fan, J. W. Liu, L. Z. Ouyang, L. C. Yang, and M. Zhu, "Lithium difluorophosphate as a promising electrolyte lithium additive for high-voltage lithium-ion batteries." *ACS Appl. Energy Mater.*, **6**, 2647 (2018).
14. J. Alvarado et al., "A carbonate-free, sulfone-based electrolyte for high-voltage Li-ion batteries." *Mater. Today*, **21**, 341 (2018).

15. A. Hofmann and T. Hanemann, "Novel electrolyte mixtures based on dimethyl sulfone, ethylene carbonate and LiPF6 for lithium-ion batteries." *J. Power Sources*, **298**, 322 (2015).
16. X.-G. Sun and C. A. Angell, "New sulfone electrolytes for rechargeable lithium batteries. Part I. Oligoether-containing sulfones." *Electrochem. Commun.*, **7**, 261 (2005).
17. E. Nanini-Maury, J. Swiatowska, A. Chagnes, S. Zanna, P. Tran-Van, P. Marcus, and M. Cassir, "Electrochemical behavior of sebaconitrile as a cosolvent in the formulation of electrolytes at high potentials for lithium-ion batteries." *Electrochim. Acta*, **115**, 223 (2014).
18. A. Hofmann, M. Schulz, S. Indris, R. Heinzmann, and T. Hanemann, "Mixtures of ionic liquid and sulfolane as electrolytes for li-ion batteries." *Electrochim. Acta*, **147**, 704 (2014).
19. P. Hilbig, L. Ibing, R. Wagner, M. Winter, and I. Cekic-Laskovic, "Ethyl methyl sulfone-based electrolytes for lithium ion battery applications." *Energies*, **10**, 1312 (2017).
20. G. C. Yan, X. H. Li, Z. X. Wang, H. J. Guo, W. J. Peng, Q. Y. Hu, and J. X. Wang, "Fluorinated solvents for high-voltage electrolyte in lithium-ion battery." *J. Solid States Electrochem.*, **21**, 1589 (2017).
21. G. Marcou, B. Flamme, G. Beck, A. Chagnes, O. Mokshyna, D. Horvath, and A. Varnek, "In silico design of novel electrolytic solvents." *Mol. Inf.*, **38**, 1900014 (2019).
22. B. Flamme, M. Haddad, P. Phansavath, V. Ratovelomanana-Vidal, and A. Chagnes, "Anodic stability of new sulfone-based electrolytes for lithium-ion batteries." *Chem. Electro. Chem.*, **5**, 2279 (2018).
23. J. Świątowska-Mrowiecka, V. Maurice, S. Zanna, L. Klein, and P. Marcus, "XPS study of Li ion intercalation in V_2O_5 thin films prepared by thermal oxidation of vanadium metal." *Electrochim. Acta*, **52**, 5644 (2007).
24. E. Markevich, G. Salitra, and D. Aurbach, "Fluoroethylene carbonate as an important component for the formation of an effective solid electrolyte interphase on anodes and cathodes for advanced li-ion batteries." *ACS Energy Lett.*, **2**, 1337 (2017).
25. L. Ma, S. L. Glazier, R. Petibon, J. Xi, J. M. Peters, Q. Liu, J. Allen, R. N. C. Doig, and J. R. Dahn, "A guide to ethylene carbonate-free electrolyte making for li-ion cells." *J. Electrochem. Soc.*, **164**, A5008 (2017).
26. R. Petibon, J. Xia, L. Ma, M. Bauer, K. Nelson, and J. R. Dahn, "Electrolyte system for high voltage li-ion cells." *J. Electrochem. Soc.*, **163**, A2571 (2016).
27. M. Klett, P. Svens, C. Tengstedt, A. Seyeux, J. Świątowska, G. Lindbergh, and R. Wreland Lindstrom, "Uneven film formation across depth of porous graphite electrodes in cycled commercial Li-ion batteries." *J. Phys. Chem. C*, **119**, 90 (2015).
28. B. Tian, J. Światowska, V. Maurice, S. Zanna, A. Seyeux, and P. Marcus, "Binary iron-chromium oxide as negative electrode for lithium-ion micro-batteries—spectroscopic and microscopic characterization." *Appl. Surf. Sci.*, **353**, 1170 (2015).
29. F. Liao, J. Światowska, V. Maurice, A. Seyeux, L. H. Klein, S. Zanna, and P. Marcus, "Influence of the electrolyte on chemical and morphological modifications of iron sulfide thin film negative electrode." *Phys. Chem. Chem. Phys.*, **17**, 619 (2015).
30. C. Pereira-Nabais, J. Światowska, M. Rosso, F. Ozanam, A. Seyeux, A. Gohier, P. Tran-Van, M. Cassir, and P. Marcus, "Effect of lithiation potential and cycling on chemical and morphological evolution of si thin film electrode studied by tof-sims." *ACS Appl. Mat. Interf.*, **6**, 13023 (2014).
31. Y. Chu, Y. Shen, F. Guo, X. Zhao, Q. Dong, Q. Zhang, W. Li, H. Chen, Z. Luo, and L. Chen, "Advanced characterizations of solid electrolyte interphases in lithium-ion batteries." *Electrochem. Energ. Rev*, DOI:10.1007/s41918-019-00058-y (2019).
32. S. Dapoz, N. Betz, M.-J. Guittet, and A. L. Moel, "ESCA characterization of heparin-like fluoropolymers obtained by functionalization after grafting induced by swift heavy ion irradiation." *Nucl. Instrum. Methods Phys. Res. Sec. B*, **105**, 120 (1995).
33. J. Świątowska, V. Lair, C. Pereira-Nabais, G. Cote, P. Marcus, and A. Chagnes, "XPS, XRD and SEM characterization of a thin ceria layer deposited onto graphite electrode for application in lithium-ion batteries." *Appl. Surf. Sci.*, **257**, 9110 (2011).
34. V. Sharova, A. Moretti, T. Diemant, A. Varzi, R. J. Behm, and S. Passerini, "Comparative study of imide-based Li salts as electrolyte additives for Li-ion batteries." *J. Power Sources*, **375**, 43 (2018).
35. B. Philippe, R. Dedryvère, M. Gorgoi, H. Rensmo, D. Gonbeau, and K. Edström, "Improved performances of nanosilicon electrodes using the salt LiFSI: a photoelectron spectroscopy study." *J. Am. Chem. Soc.*, **135**, 9829 (2013).
36. J. Demeaux, E. De Vito, M. Le Digabel, H. Galiano, B. Claude-Montigny, and D. Lemordant, "Dynamics of $Li_4Ti_5O_{12}$/sulfone-based electrolyte interfaces in lithium-ion batteries." *Phys. Chem. Chem. Phys.*, **16**, 5201 (2014).
37. Y. Diao, K. Xie, S. Xiong, and X. Hong, "Insights into Li-S battery cathode capacity fading mechanisms: irreversible oxidation of active mass during cycling." *J. Electrochem. Soc.*, **159**, A1816 (2012).
38. S. Li, X. Xu, X. Shi, B. Li, Y. Zhao, H. Zhang, Y. Li, W. Zhao, X. Cui, and L. Mao, "Composition analysis of the solid electrolyte interphase film on carbon electrode of lithium-ion battery based on lithium difluoro(oxalate)borate and sulfolane." *J. Power Sources*, **217**, 503 (2012).
39. X. Zheng, T. Huang, Y. Pan, W. Wang, G. Fang, and M. Wu, "High-voltage performance of $LiNi_{1/3}Co_{1/3}Mn_{1/3}O_2$/graphite batteries with di(methylsulfonyl) methane as a new sulfone-based electrolyte additive." *J. Power Sources*, **293**, 196 (2015).
40. A. Nytén, M. Stjerndahl, H. Rensmo, H. Siegbahn, M. Armand, T. Gustafsson, K. Edström, and J. O. Thomas, "Surface characterization and stability phenomena in Li_2FeSiO_4 studied by PES/XPS." *J. Mater. Chem.*, **16**, 3483 (2006).
41. D. Ensling, M. Stjerndahl, A. Nytén, T. Gustafsson, and J. O. Thomas, "A comparative XPS surface study of Li_2FeSiO_4/C cycled with LiTFSI- and LiPF6-based electrolytes." *J. Mater. Chem.*, **19**, 82 (2009).
42. A. M. Andersson, M. Herstedt, A. G. Bishop, and K. Edström, "The influence of lithium salt on the interfacial reactions controlling the thermal stability of graphite anodes." *Electrochim. Acta*, **47**, 1885 (2002).
43. H. Shin, J. Park, A. M. Sastry, and W. Lu, "Effects of fluoroethylene carbonate (FEC) on anode and cathode interfaces at elevated temperatures." *J. Electrochem. Soc.*, **162**, A1683 (2015).
44. A. Chagnes and J. Swiatowska, "Electrolyte and solid-electrolyte interphase layer in lithium-ion batteries." in *Lithium Ion Batteries-New Developments*, ed. I. Belharouak (Intech, Amsterdam) pp 158–64 (2012).
45. B. P. Balbuena and X. Wuang, in *Lithium Ion Batteries—Solid Electrolyte Interphase* (Imperial College Press, London) (2004).
46. J. Swiatowska-Mrowiecka, V. Maurice, S. Zanna, L. Klein, and P. Marcus, "XPS study of Li ion intercalation in V_2O_5 thin films prepared by thermal oxidation of vanadium metal." *Electrochim. Acta*, **52**, 5644 (2007).
47. J. Swiatowska-Mrowiecka, S. de Diesbach, V. Maurice, S. Zanna, L. Klein, E. Briand, I. Vickridge, and P. Marcus, "Li-ion intercalation in thermal oxide thin films of MoO_3 as studied by XPS, RBS, and NRA." *J. Phys. Chem. C*, **112**, 11050 (2008).
48. P. Verma, P. Maire, and P. Novák, "A review of the features and analyses of the solid electrolyte interphase in Li-ion batteries." *Electrochim. Acta*, **55**, 6332 (2010).
49. M. B. Armand, M. J. Duclot, and P. Rigaud, "Polymer solid electrolytes: Stability domain." *Solid State Ionics*, **3–4**, 429 (1981).
50. M. Nakayama, S. Wada, S. Kuroki, and M. Nogami, "Factors affecting cyclic durability of all-solid-state lithium polymer batteries using poly(ethylene oxide)-based solid polymer electrolytes." *Energy Environ. Sci.*, **3**, 1995 (2010).
51. A. M. Andersson and K. Edström, "Chemical composition and morphology of the elevated temperature SEI on graphite." *J. Electrochem. Soc.*, **148**, A1100 (2001).
52. H. Bryngelsson, M. Sjterndahl, T. Gustafsson, and K. Edström, "How dynamic is the SEI?" *J. Power Sources*, **174**, 970 (2007).
53. G. G. Eshetu, T. Diemant, S. Grugeon, R. J. Behm, S. Laruelle, M. Armand, and S. Passerini, "In-depth interfacial chemistry and reactivity focused investigation of lithium–imide- and lithium–imidazole-based electrolytes." *ACS Appl. Mater. Interfaces*, **8**, 16087 (2016).